Journal of Sound and Vibration (1972) **22** (2), 221–232

SOUND PROPAGATION IN DUCT SHEAR LAYERS

P. N. SHANKAR

Department of Aerospace Engineering,
University of Maryland, College Park, Maryland 20742, *U.S.A.*

(*Received* 1 *February* 1972)

The propagation of sound in a two-dimensional inviscid shear layer is considered for given initial sound pressure profiles. The eigenvalue problem resulting from an assumption of separable solutions of the form $\phi(y)\exp\{ik(\beta x - ct)\}$, first obtained by Pridmore-Brown, is solved numerically. It is shown that although the resulting eigenfunctions cannot be proven to be orthogonal or complete, they can be combined by a least total error squared method to give a good representation of the initial pressure profile. The acoustic pressure in the duct is then easily calculated. The results verify all the predictions made in an earlier perturbation calculation. Moreover, they show that the refraction effect gets saturated at high subsonic Mach numbers and at high frequencies. The present technique may be used, if necessary, with impedance boundary conditions at the duct walls.

1. INTRODUCTION

The geometry of the problem under study is shown in Figure 1. Sound is generated at a station $x = 0$ in a semi-infinite duct of width $2b$. The duct contains an inviscid moving medium whose steady velocity $U(y)$ is axial and is a function of y alone. The propagation of sound in such a non-uniform medium is governed by the following linearized equations:

$$\frac{1}{c^2}\left(\frac{\partial p}{\partial t} + U(y)\frac{\partial p}{\partial x}\right) + \rho_\infty\left(\frac{\partial u}{\partial x} + \frac{\partial v}{\partial y}\right) = 0, \tag{1a}$$

$$\frac{\partial u}{\partial t} + U(y)\frac{\partial u}{\partial x} + v\frac{dU}{dy} = -\frac{1}{\rho_\infty}\frac{\partial p}{\partial x}, \tag{1b}$$

$$\frac{\partial v}{\partial t} + U(y)\frac{\partial v}{\partial x} = -\frac{1}{\rho_\infty}\frac{\partial p}{\partial y}, \tag{1c}$$

where p, u, and v are the acoustic quantities, ρ_∞ is the ambient density, $U(y)$ is the given axial velocity and $c = \sqrt{\gamma RT_\infty}$ is the ambient sound speed. The normal velocity v has to vanish at the wall.

In a 1958 paper, Pridmore-Brown [1] attempted to get a solution to the equations (1) by assuming separation of variables. He assumed that the pressure, for example, had a solution of the form

$$p = \phi(y)\exp\{ik(\beta x - ct)\}, \tag{2}$$

where $k = \omega/c$ is the given undisturbed wave number, and β is an unknown constant. If u and v are also assumed to have solutions of the same form, equations (1a), (1b), and (1c) reduce to an eigenvalue problem for β:

$$\frac{d^2\phi}{dy^2} + \frac{2\beta(dM/dy)}{(1-\beta M)}\frac{d\phi}{dy} + k^2[(1-\beta M)^2 - \beta^2]\phi = 0, \tag{3a}$$

$$\left(\frac{d\phi}{dy}\right)_{y=0} = \left(\frac{d\phi}{dy}\right)_{y=2b} = 0. \tag{3b}$$

Here $M(y) = U(y)/c$ is the subsonic Mach number of the steady uniform flow.

In order to proceed further, Pridmore-Brown studied two particular $M(y)$ profiles, the linear profile and a turbulent 1/7th power profile. He obtained solutions for the lowest mode in each case, in the limit of infinitely weak shear, by a WKB type method. However, for the 1/7th power mean velocity profile, with an infinite gradient at the wall, the solution broke down in that neighbourhood.

Mungur and Gladwell [2] studied the same eigenvalue problem, equations (3), but by a straightforward numerical technique. Again they restricted themselves to the lowest even modes and always to cases where β was real. No indication was given as to what these solutions represented.

The major thesis of an earlier paper [3] was that studies such as the above, restricted to calculating lowest modes, were inadequate. The modes in themselves represent nothing more than particular solutions to the governing equations. They acquire a meaning only if they can and are used to represent a given initial pressure profile; they may then predict the acoustic pressure distribution everywhere in the duct. However, the eigenvalue problem represented by equations (3) is not a standard eigenvalue problem of the Sturm–Liouville type; the eigenvalue appears in a non-linear fashion and is not restricted to the $\phi(y)$ term in the equation. None of the standard theorems on completeness, orthogonality, etc. appear to be obviously applicable to this problem.

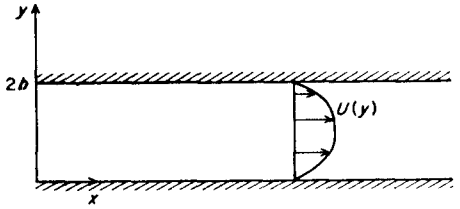

Figure 1. Sound propagation in a duct of width $2b$ containing a shear flow $U(y)$.

It was to avoid these difficulties and the assumption of spatial separability that a perturbation technique was used in Shankar (1971) to solve the complete initial boundary value problem. The generating pressure at $x = 0$ was taken to be given by $p(0,y,t) = p_0 H(t) \exp(-i\omega t)$ where $H(t)$ is the unit step function and the flow Mach number was assumed to be weakly sheared, $M(y) = \epsilon M^{(1)}(y)$. It was then shown that for large time and for stations far from the initial wave front the acoustic pressure is given by

$$p(x,y,t) = p_0 \exp\left\{-i\omega\left[t - \frac{x}{c}\left(1 - \frac{\epsilon \tilde{a}_0}{2b}\right)\right]\right\} + \epsilon p_0 \sum_{n=1}^{\infty} \frac{8}{\pi^2} \frac{\tilde{a}_n}{bn^2} \left(\frac{b^2\omega^2}{c^2}\right) \times$$

$$\times \cos\left(\frac{n\pi y}{2b}\right) e^{-i\omega t}\left[\exp\left\{ix\left(\frac{\omega^2}{c^2} - \frac{n^2\pi^2}{4b^2}\right)^{1/2}\right\} - \exp\left(\frac{i\omega x}{c}\right)\right] + 0(\epsilon^2), \quad (4)$$

where $\tilde{a}_n$ is the Fourier coefficient of the Mach number profile:

$$\tilde{a}_n = \int_0^{2b} M^{(1)}(y) \cos\left(\frac{n\pi y}{2b}\right) dy. \quad (5)$$

In deriving the solution a secular term had to be corrected by a slight straining of the axial coordinate. Luckily it was possible to do this by inspection; this accounts for the ϵ term in the exponential of the lowest-order term in equation (4). The solution shows that in this limit one can treat the sound as being convected by the mean axial velocity and then being refracted by the shear about this mean value. Note also that the solution (4) is indeed separable in the spatial coordinates. In reference [3] detailed calculations are presented to show interesting

effects such as the dependence of the pressure on the axial distance from the source, a cut-off phenomenon, and the existence of standing wave type patterns.

While the perturbation calculation clearly demonstrated the importance of studying the complete boundary value problem, it suffered from the major weakness that the calculation failed when the refractive effects became sufficiently large. In particular, the linear dependence on Mach number and quadratic dependence on frequency limited the calculations to low Mach number and frequency. The present paper is an attempt to overcome these limitations.

Based on our knowledge of the weak shear limit, we shall assume, following Pridmore-Brown, that the solution is indeed separable in all the variables. The eigenvalue equation (3) then determines the solution to the problem. Unlike Pridmore-Brown and Mungur and Gladwell, however, our interest is not in the lowest modes which are in themselves meaningless; the objective is to solve the complete boundary value problem for a given source pressure distribution. In order to do this we shall assume, in the absence of proof, that (i) there exists a lowest eigenvalue β_0, (ii) there exists a set of distinct higher eigenvalues β_n, and (iii) the corresponding eigenfunctions ϕ_n are complete.

The pressure in the duct may then be represented as follows:

$$p(x,y,t) = \sum_{n=0}^{\infty} a_n \phi_n(y) \exp\{ik(\beta_n x - ct)\}. \tag{6}$$

The β_n and $\phi_n(y)$ are linearly independent eigenvalues and eigenfunctions and the a_n are "amplitude coefficients". The coefficients a_n are determined from the pressure profile at the source, $x = 0$, where the time dependence is assumed harmonic with frequency $\omega = kc$. Since the eigenfunctions are not orthogonal, at least to any known weighting function, a least total error squared method will be used to calculate the a_n.

As far as the calculation of the eigenfunctions is concerned, one might be tempted to use Pridmore-Brown's technique in order to obtain analytical results. Apart from the restriction to weak shear (which we are trying to avoid), and the failure near the walls, the labour involved in obtaining more than a few eigenfunctions would be enormous. For these reasons, we shall, reluctantly, calculate the eigenfunctions and eigenvalues by a direct numerical technique. There will then be no restriction on the frequency and on the (subsonic) Mach number of the flow.

An outline of the calculational procedure is given in section 2 and the results are discussed in section 3. It is found that the eigenfunctions are indeed capable of representing initial pressure profiles. In the limit of weak shear the present calculations verify the conclusions obtained from the perturbation calculation. The most important result, however, is that at high Mach number and frequency the refractive effect is saturated leading mainly to complicated standing wave type patterns rather than channelling towards the walls of the duct.

2. NUMERICAL METHOD

There are three basic steps to the calculation: (i) the calculation of the eigenvalues and the eigenfunctions; (ii) the calculation of the "amplitude coefficients"; (iii) the calculation of the pressure in the duct.

Step (i) is by far the major one. One has to locate a given number of independent eigenvalues and eigenfunctions. We limit ourselves to the lowest mode and the next ten significant higher modes. These appear to be sufficient for most purposes. The eigenvalues may be real or complex and the technique to locate them is slightly different in each case.

One is guided by the expectation that the eigenvalue for the shear layer case will lie close to the corresponding ones for the no flow and the uniform flow cases, i.e. close to $\{1 - n^2\pi^2/4k^2b^2\}^{1/2}$ and $[(-M_0 + \{1 - (n^2\pi^2/4k^2b^2)(1 - M_0^2)\}^{1/2})/(1 - M_0^2)]$, where M_0 is the

peak Mach number in the shear layer. In fact if both of these are real, we should expect the eigenvalue to be between the two. This is in fact what is found.

When the eigenvalue is real it is best to start with the uniform flow value for β and work towards the upper, no flow value. We pick a value of β, set $\phi(0) = 1 + i$ (since the normalizing factor is arbitrary), and $\phi'(0) = 0$, and integrate to the outer wall. If $\phi'(y = 2b)$ is not zero we go back and increase β and repeat the calculation. As soon as the sign of ϕ' changes at $y = 2b$, the step in β is reduced successively to sweep the location of the eigenvalue. When $|\phi'(y = 2b)|$ is sufficiently small ($<0{\cdot}001$) we have picked out an eigenvalue and an eigenfunction.

When the eigenvalue is complex a gradient technique is used. The error in ϕ' at $y = 2b$ is assumed to be analytic in β. From calculating the change in $\phi'(y = 2b)$ due to small changes in β one can home in on the eigenvalue.

The details of the method have been given because, at high Mach number and frequency, the eigenvalues tend to be located close to each other. A straightforward gradient approach will lead to locating the same eigenvalues over and over again, especially in the real case. One has to check that one has indeed picked the eleven lowest significant eigenvalues. This is done by counting the zeros of the eigenfunctions. The nth eigenfunction must have n zeros between $y = 0$ and $2b$. If the located eigenfunction does not have the appropriate number of zeros, it is not the one one is looking for, and the calculation has to be repeated.

The integration scheme was a fourth-order Runge–Kutta scheme with a step size of 0·02 in y/b. When the step size was cut in half no significant changes were observable.

For symmetrical velocity profiles it is sufficient to integrate to $y/b = 1$ since the eigenfunctions have to be symmetrical or antisymmetrical. For the even modes, then, $\phi'(y/b = 1) = 0$ and for the odd modes, $\phi(y/b = 1) = 0$.

Once the eigenfunctions have been calculated the coefficients a_n are calculated from the pressure distribution at $x = 0$ by at least total error squared fit. If $p(0, y, t) = p_0 g(y) \exp(-i\omega t)$, the total (error)^2 over M points along y is minimized provided

$$\sum_{l=0}^{N-1} \sum_{k=1}^{M} \{\phi_l(y_k)\phi_j(y_k)\} a_l = \sum_{k=1}^{M} p_0 g(y_k)\phi_j(y_k), \qquad j = 0 \ldots (N-1). \tag{7}$$

The a_n are then given by a matrix inversion. In the calculations presented, the error was minimized over 51 points in the range $0 \leqslant y/b \leqslant 1$ for symmetrical velocity and initial pressure profiles and over 101 points in the range $0 \leqslant y/b \leqslant 2$ for non-symmetrical velocity profiles.

Finally the pressure is calculated for various x/b locations from the formula (6).

The complete calculational time for a given pair of kb and M_0 values ranges from 25 to 35 seconds on a UNIVAC 1108 computer with about 95% of the time going towards the calculation of the eleven eigenfunctions.

3. DISCUSSION OF RESULTS

All the eigenvalues quoted by Mungur and Gladwell [2] in their Table 1, for the lowest modes, were checked out. All these eigenvalues are real. The agreement was excellent for the linear velocity profile cases but poorer for the $M(y) = (y/b)^{1/7}$, $0 \leqslant y \leqslant b$, turbulent profile cases. Typical comparisons are shown in Figure 2. The linear cases are indistinguishable. The integration step size was halved with virtually no change in the results. We are forced to conclude that the results quoted by Mungur and Gladwell are in error in the turbulent profile cases.

The results that follow are for the turbulent mean velocity profile:

$$M(y) = \begin{cases} M_0(y/b)^{1/7} & 0 \leqslant y \leqslant b \\ M_0(2 - y/b)^{1/7} & b \leqslant y \leqslant 2b, \end{cases}$$

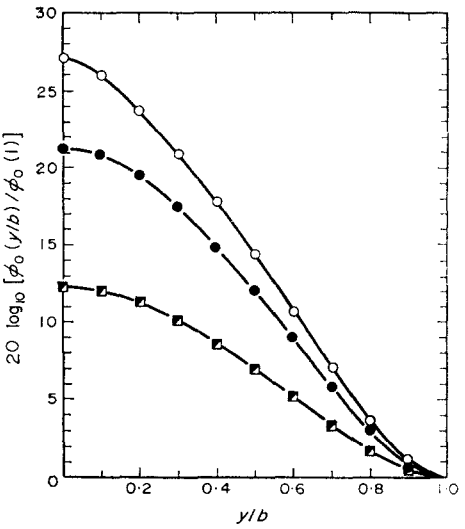

Figure 2. Comparison of lowest modes with those of Mungur and Gladwell [2]. ○, ● are for a turbulent profile with $M_0 = 0{\cdot}3, kb = 20$; □, ■ are for a linear profile with $M_0 = 0{\cdot}3, kb = 10$. The open symbols represent the present calculation. The corresponding eigenvalues are: β_0 (turbulent case) = 0·81192, 0·8033; β_0 (linear) = 0·91943, 0·9194.

and an initial pressure profile $p(0, y, t) = p_0 \exp(-i\omega t)$, unless otherwise stated. In all the following figures only six points in the pressure profile are marked with symbols; the curves, however, pass through five other unmarked calculated points.

Figure 3(a) shows typical mode shapes for $M_0 = 0{\cdot}3$ and $kb = 10$. The lowest mode ϕ_0 shows the typical distortion characteristic of refraction. However, the first even complex mode ϕ_8 (corresponding to the first even complex eigenvalue) shows little distortion from the no flow case. The real and imaginary parts are not quite equal or quite in phase but they are almost so. This is fairly typical—the greatest distortions occur is the lowest mode, ϕ_0, whilst the higher modes do not contribute much to the refractive effect (at least directly!). The location in the complex β plane of the eleven lowest even eigenvalues is shown in Figure 3(b), for $kb = 10$ and $M_0 = 0{\cdot}1$ and $M_0 = 0{\cdot}3$. There are four propagating modes in each case. The effect of increasing Mach number is of course to increase the propagation speed of each

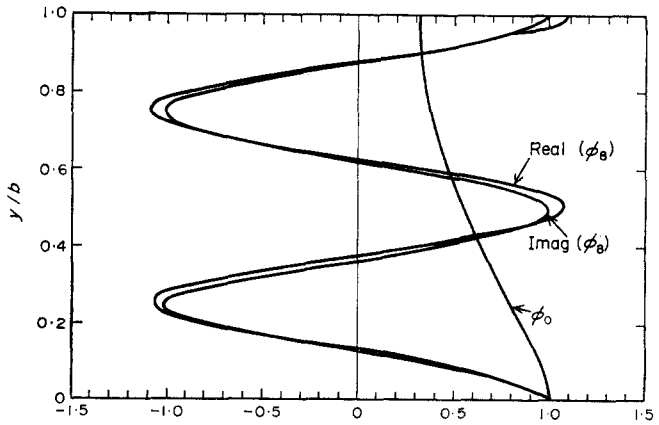

Figure 3(a). Mode shapes for $M_0 = 0{\cdot}3, kb = 10$. ϕ_0 is the lowest mode with equal real and imaginary parts and ϕ_8 is the first even complex mode. The corresponding eigenvalues are: $\beta_0 = 0{\cdot}79980$, $\beta_8 = -0{\cdot}28378 + 0{\cdot}73477i$.

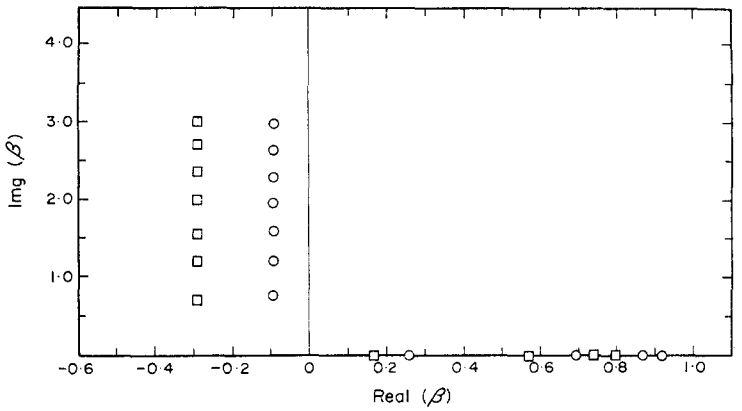

Figure 3(b). Location of the lowest eleven even eigenvalues in the complex plane. $kb = 10$; ○, $M_0 = 0{\cdot}1$ □, $M_0 = 0{\cdot}3$.

mode, i.e. the eigenvalues are shifted to the left. The complex eigenvalues display another typical feature. They tend to have approximately the same wavelength but increasing attenuation factors. These features are of help in locating distinct eigenvalues. Returning to Figure 3(a), we note that the number of zeros of each ϕ_n in $0 \leqslant y \leqslant 2b$ is equal to n.

The details of a calculation are shown in Tables 1 and 2. The peak Mach number is 0·3 and the frequency parameter kb is equal to 5. Since the velocity profile is symmetric the modes are symmetric or antisymmetric about $y = b$. As we are going to calculate the propagation of sound from an initially plane (symmetrical about $y = b$) sound pressure profile, we calculate the lowest eleven symmetrical modes, ϕ_0 to ϕ_{20}. Table 1 shows the corresponding eigenvalues indicating two propagating modes. It is to be noted that the amplitudes a_n decay uniformly and rapidly with n. This is an important consideration if the calculation is to be useful. With these coefficients, Table 2 shows the capability of the functions ϕ_n to represent an initially uniform profile. The exact result is that the real part of 1 is 1 and its imaginary part is 0. Although only 10 points are shown in Table 2, the error is no worse at 40 other points in the interval $0 \leqslant y/b \leqslant 1$. As the error is at worst 2 parts in 1000, the representation is clearly adequate.

The results of the present calculation are compared with those of the perturbation calculation in Figures 4(a) and 4(b). At a Mach number of 0·1 and frequency of $kb = 5$, agreement

TABLE 1

$kb = 5$, $M_0 = 0{\cdot}3$

n	β_n	a_n
0	0·79314	0·57679 − 0·57670i
2	0·57184	−0·06694 + 0·06698i
4	−0·28672 + 0·73219i	−0·00570 + 0·00554i
6	−0·29167 + 1·62556i	−0·00211 + 0·00210i
8	−0·29475 + 2·36487i	−0·00076 + 0·00080i
10	−0·29670 + 3·06372i	−0·00043 + 0·00042i
12	−0·29787 + 3·74512i	−0·00023 + 0·00023i
14	−0·29850 + 4·41747i	−0·00016 + 0·00014i
16	−0·29874 + 5·08476i	−0·00010 + 0·00009i
18	−0·29872 + 5·74920i	−0·00007 + 0·00006i
20	−0·29852 + 6·41218i	−0·00005 + 0·00004i

TABLE 2

$kb = 5,\ M_0 = 0{\cdot}3$

y/b	Real part of 1	Imaginary part of 1
0·0	1·00213	−0·00023
0·1	0·99966	0·00015
0·2	0·99996	−0·00009
0·3	1·00015	0·00006
0·4	0·99981	−0·00003
0·5	1·00021	0·00001
0·6	0·99979	0·00000
0·7	1·00022	−0·00001
0·8	0·99978	0·00002
0·9	1·00023	−0·00002
1·0	0·99977	0·00002

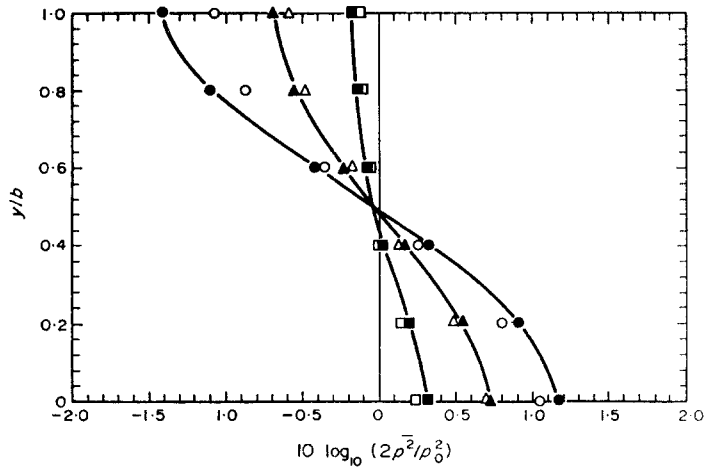

Figure 4(a). Comparison with the perturbation calculation (Shankar [3]). Open symbols represent the present calculation. $kb = 5$; $M_0 = 0{\cdot}1$; ○, $x/b = 20$; □, $x/b = 80$; △, $x/b = 140$.

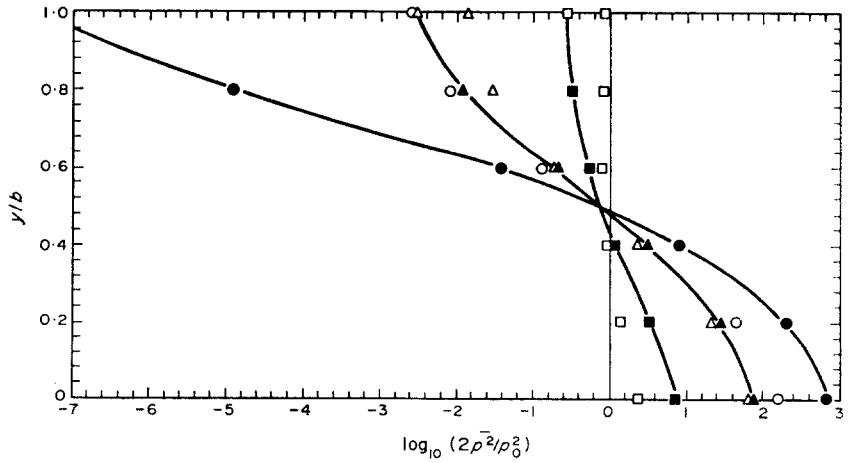

Figure 4(b). Comparison with the perturbation calculation (Shankar [3]). Open symbols represent the present calculation. $kb = 5$; $M_0 = 0{\cdot}3$; ○, $x/b = 20$; □, $x/b = 80$; △, $x/b = 140$.

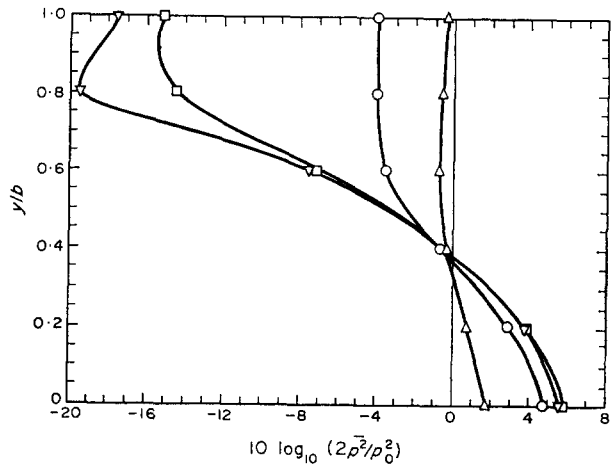

Figure 5(a). Standing wave type patterns created by interference of propagating modes. $kb = 10$; $M_0 = 0{\cdot}3$; ○, $x/b = 40$; □, $x/b = 60$; △, $x/b = 120$; ▽, $x/b = 200$.

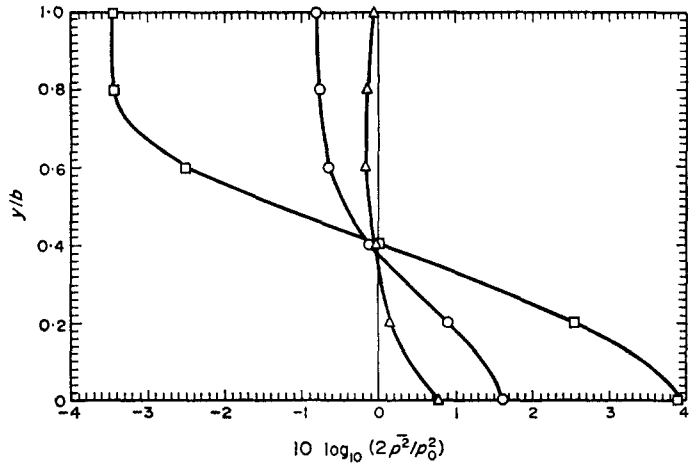

Figure 5(b). The effect of increasing Mach number at a given location, $x/b = 100$, and at a given frequency, $kb = 10$. ○, $M_0 = 0{\cdot}1$; □, $M_0 = 0{\cdot}3$; △, $M_0 = 0{\cdot}5$.

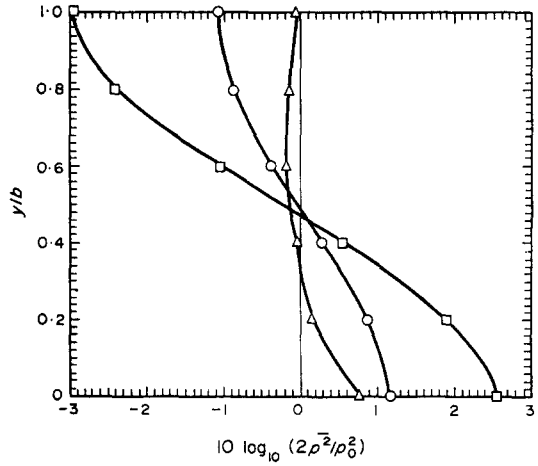

Figure 5(c). The effect of increasing frequency at a given location, $x/b = 100$, and a given Mach number, $M_0 = 0{\cdot}5$. ○, $kb = 3{\cdot}5$; □, $kb = 5$; △, $kb = 10$.

is quite good. At a higher Mach number of 0·3 the agreement is much poorer, but the trends are again in agreement (e.g. the wall pressure is lower at $x/b = 140$ than at $x/b = 20$, but higher than at $x/b = 80$). Note that the dB scale exaggerates any differences when the r.m.s. pressure falls below $p_0/\sqrt{2}$. All the general features predicted by the perturbation calculation have been verified by the present calculation.

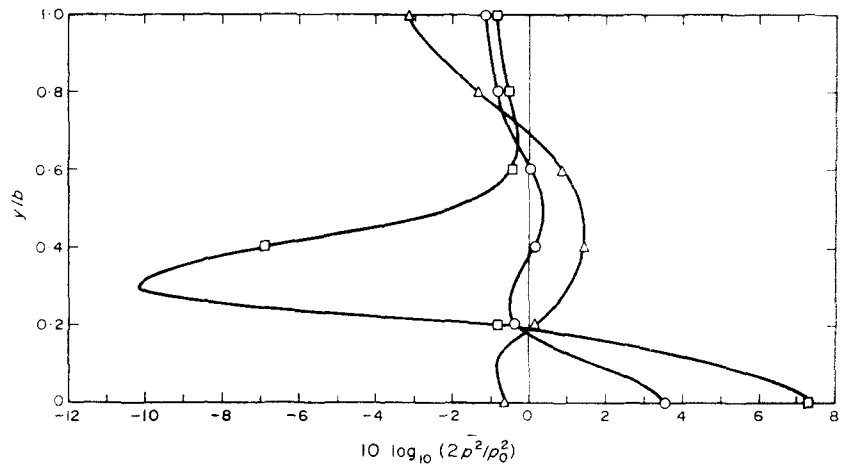

Figure 6. Effect of high Mach number and frequency. There are nine propagating modes in this case. $M_0 = 0{\cdot}8$; $kb = 20$; ○, $x/b = 100$; □, $x/b = 140$; △, $x/b = 180$.

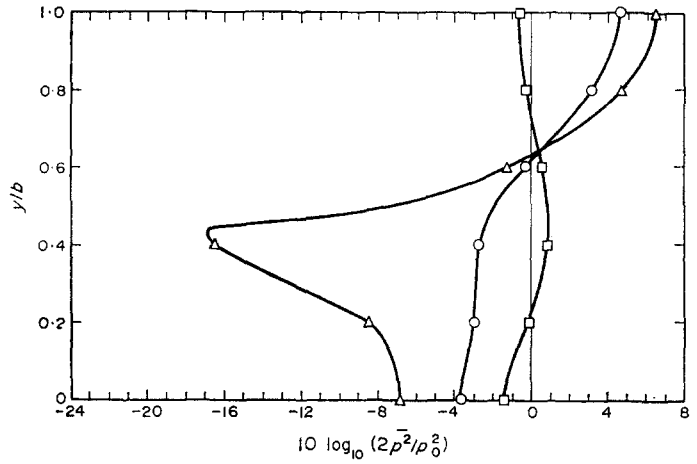

Figure 7. Sound propagation against the flow. The channelling is towards the center. $M_0 = -0{\cdot}5$; $kb = 5$; ○, $x/b = 60$; □, $x/b = 80$; △, $x/b = 120$.

Figures 5(a), 5(b), and 5(c) show typical refraction effects. When there are a number of propagating modes, they interfere with one another to create complicated standing wave type patterns. At $kb = 10$ and $M_0 = 0{\cdot}3$, there are four propagating modes; the pressure does tend to build up at the wall but it is oscillatory in x. At a given location, the effect of increasing the Mach number is initially to increase the refractive effect and then to decrease it. Similarly the effect of increasing frequency is an initial increase followed by a decrease. Of course at a different x/b location the results are not necessarily the same, but invariably the refractive effect does not increase without bound with increasing kb and M_0.

The chief failing of the perturbation calculation was its inability to handle high subsonic Mach numbers, and high frequency. No estimates could be made of what occurred when the refractive effects became large. The present calculation clarifies this issue. Figure 6 shows calculations at a high Mach number $M_0 = 0{\cdot}8$ and a high frequency of $kb = 20$. There are nine propagating modes in this case and while the interference patterns are, needless, more complicated, the magnitude of the wall pressure build up is in no way enormous.

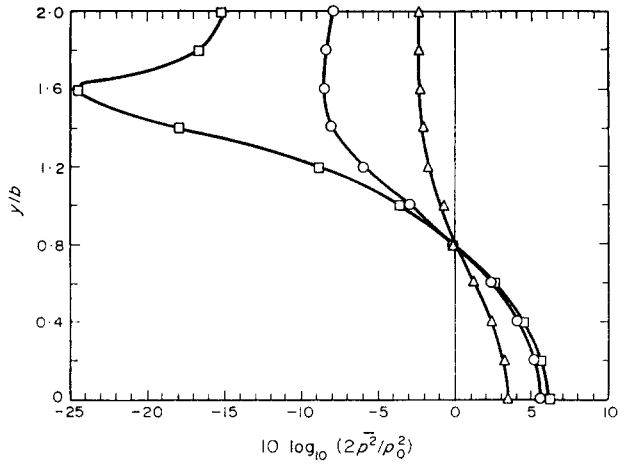

Figure 8. The case of a linear velocity profile: $M(y) = M_0(y/b), 0 \leqslant y \leqslant 2b$. $M_0 = 0{\cdot}2$; $kb = 3{\cdot}5$; ○ $x/b = 20$; □, $x/b = 80$; △, $x/b = 200$.

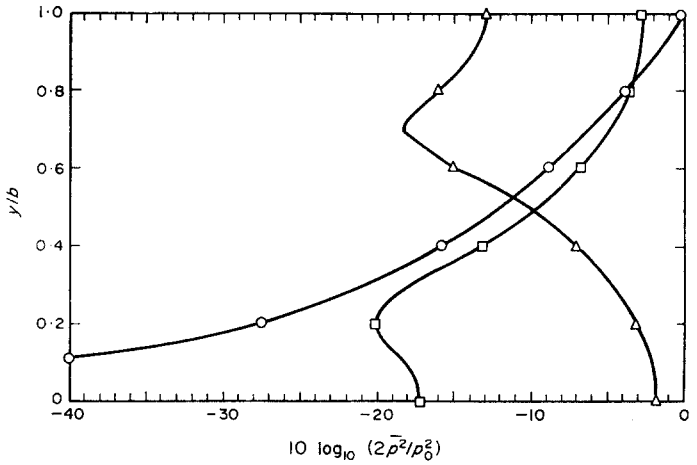

Figure 9. An initially non-uniform pressure profile: $p(0,y,t) = p_0(y/b)^2 \exp(-i\omega t), 0 \leqslant y \leqslant b$. $M_0 = 0{\cdot}3$; $kb = 5$; ○, $x/b = 0$; □, $x/b = 40$; △, $x/b = 60$.

There are two competing effects as the frequency and Mach number are increased. On the one hand the lowest mode ϕ_0 gets more and more distorted tending to enhance the build up towards the wall. On the other hand more and more of the higher modes, which detract from the wall build up, begin to propagate. As ϕ_0 gets more distorted the amplitudes a_n of the higher modes required to represent an initially uniform pressure profile increase. These two effects tend to balance each other. Thus at high frequency and Mach number the net effect is mainly a more complicated interference pattern in the pressure, rather than increased pressure build up at the wall.

Figure 7 shows the channelling towards the centre of the duct when the sound propagates against the flow. In this case, of course, the real eigenvalues are greater than 1 (propagation velocities less then c).

The results for a linear velocity profile are shown in Figure 8. In this case the eigenfunctions are neither symmetrical nor antisymmetrical about $y/b = 1$. We have therefore to use the lowest eleven eigenfunctions, ϕ_0 to ϕ_{10}, to represent the initial profile. In carrying out the integrations, the range has to be $0 \leqslant y/b \leqslant 2$ rather than $0 \leqslant y/b \leqslant 1$ as in the symmetrical

TABLE 3

$kb = 5,\ M_0 = 0{\cdot}3$

y/b	Real part of $(y/b)^2$	Imaginary part of $(y/b)^2$
0·0	0·00182	0·0008
0·1	0·00780	−0·00001
0·2	0·04216	−0·00004
0·3	0·08791	0·00009
0·4	0·16200	−0·00014
0·5	0·24813	0·00019
0·6	0·36167	−0·00024
0·7	0·48869	0·00029
0·8	0·64046	−0·00034
0·9	0·81261	0·00040
1·0	0·96913	−0·00038

velocity profile cases. Again, the eigenfunctions give an adequate representation of the initial profile.

Finally we consider the case of an initially non-uniform pressure profile. Figure 9 shows the results when the pressure at $x = 0$ is given by

$$p(0, y, t) = p_0(y/b)^2 \exp(-i\omega t), \qquad 0 \leqslant y/b \leqslant 1$$

and is symmetrical about $y/b = 1$. The eigenvalues and eigenfunctions are the same as those given in Table 1. The amplitude coefficients a_n are, of course, different. In fact, in this case a_2 is slightly larger than a_0. The other coefficients decay rapidly. Table 3 shows the deviation of the initial profile from $(y/b)^2$. The representation is not quite as good as in the uniform profile case but is still adequate. Note, again, that the errors are no greater at 40 other points in the interval $0 \leqslant y/b \leqslant 1$.

4. CONCLUSION

The purpose of this paper was to show that the eigenvalues and eigenfunctions resulting from Pridmore-Brown's eigenvalue problem could in fact be used to solve the problem of sound propagation in duct shear layers. From the calculations presented, it is clear that the eigenfunctions are capable of representing given initial pressure distributions; one would venture to guess that the eigenfunctions are indeed complete. In the absence of orthogonality, we have shown that coefficients a_n may be calculated by a least total error squared method. The rapid decay of the amplitude coefficients makes the calculation a practical one. However, it is clear that the lowest modes in themselves may give an erroneous picture of the pressure distribution in the duct. One has to consider the complete boundary value problem.

Comparison with the perturbation calculation shows that all the general features indicated by the latter are correct. When the refractive effect becomes large at high Mach number and frequency, however, the present calculations show how the effect tends to get saturated. The distortion of the lowest mode is balanced by a greater number of propagating modes with larger amplitude coefficients. This clears up the major question raised by the perturbation calculation.

The calculations considered here dealt with hard walled ducts. The technique described in this paper could, if necessary, be used with impedance boundary conditions at the walls.

ACKNOWLEDGMENT

I would like to thank Professor Holt Ashley for discussions regarding this problem and for encouragement regarding the solution. This research was supported by a grant from the Minta Martin Fund. The computer time was supported by NASA Grant NsG-398 to the Computer Science Center of the University of Maryland.

REFERENCES

1. D. C. PRIDMORE-BROWN 1958 *Journal of Fluid Mechanics* **4**, 393–406. Sound propagation in a fluid flowing through an attenuating duct.
2. P. MUNGUR and G. M. L. GLADWELL 1969 *Journal of Sound and Vibration* **9**, 28–48. Acoustic wave propagation in a sheared fluid contained in a duct.
3. P. N. SHANKAR 1971 *Journal of Fluid Mechanics* **47**, 81–91. On acoustic refraction by duct shear layers.